separations

MDPI

Article

Application of Calcium Alginate Spheres Modified with 2,4-Dinitrophenylhydrazine During the Determination of Fatty Aldehydes in Edible Oils by HPLC-DAD

F. Esmeralda Santiago-Martinez [1], Jose A. Rodriguez [1], Eva M. Santos [1], Alicia C. Mondragon-Portocarrero [2] and Jorge Lopez-Tellez [1,*]

[1] Area Academica de Quimica, Universidad Autonoma del Estado de Hidalgo, Carr. Pachuca-Tulancingo Km. 4.5, Mineral de la Reforma 42184, Hidalgo, Mexico; sa276899@uaeh.edu.mx (F.E.S.-M.); josear@uaeh.edu.mx (J.A.R.); emsantos@uaeh.edu.mx (E.M.S.)

[2] Laboratorio de Higiene, Inspeccion y Control de Alimentos, Departamento de Quimica Analitica Nutricion y Bromatologia, Universidad de Santiago de Compostela, 27002 Lugo, Spain; alicia.mondragon@usc.es

* Correspondence: lo319035@uaeh.edu.mx; Tel.: +52-(771)-717-2000 (ext. 40101)

Abstract

Saturated fatty aldehydes are products from lipid oxidation that negatively affect the organoleptic properties and nutritional quality of food and represent a risk to human health. For this reason, they are frequently used as indicators of oxidation in food safety. Usually, their determination is carried out by derivatization using an excess of 2,4-dinitrophenylhydrazine (DNPH), but the excessive use of derivatizing agents requires a high proportion compared to the analyte concentration to ensure a complete reaction, which causes interferences and limits the chromatographic separation of derivatized products. In this context, the encapsulation of DNPH in alginate spheres is proposed to determine aldehydes concentration in edible vegetable oil samples, allowing the gradual release of DNPH to form the corresponding hydrazones, which were subsequently separated and analyzed by HPLC-DAD. The proposed method was optimized by a Taguchi $L_9(3^4)$ experimental design, validated, and applied for the determination of aldehydes in edible oils. Limits of detection in the intervals of 0.77 to 1.41 mg L^{-1} were obtained with adequate precision (expressed as relative standard deviation < 10%), which are suitable values for monitoring lipid oxidation in foods The proposed methodology represents a viable alternative to apply in quality control studies and lipid degradation profiles.

Keywords: aldehydes; 2,4-dinitrophenylhydrazine encapsulation; alginate sphere; edible vegetable oils

Academic Editor: Alberto Barbiroli

Received: 15 January 2026
Revised: 13 February 2026
Accepted: 14 February 2026
Published: 21 February 2026

1. Introduction

Edible vegetable oils are obtained from several seeds and fruits [1]. These oils present a high content of unsaturated fatty acids, becoming an important source of energy apart from some of them being essential because of their participation in the regulation of physiological functions [2–4]. Nevertheless, fatty acids undergo degradation processes [5,6], with autooxidation being particularly relevant, causing deterioration of flavor, aroma, color, texture, and appearance and decreasing nutritional value [1]. The oxidation of fatty acids occurs during both storage and processing and is favored by exposure to oxygen, light, and high temperature [7,8]. This process leads to the formation of degradation products, such as hydroperoxides, ketones, organic acids, alcohols, and aldehydes [3,5,9]. The latter stand

out as the most abundant compounds, and their formation is closely related to the original fatty acid profile.

The main aldehydes formed are aliphatic aldehydes, α, β-unsaturated aldehydes, and oxygenated aldehydes [2,8,10]. Although adverse health effects, including mutagenic [3], genotoxic [8,11] and carcinogenic effects [7], have been primarily associated with unsaturated aldehydes, saturated aliphatic aldehydes have also been attributed to toxic properties in the body, such as lung problems, and a relationship with diverse types of cancer [5,8]. In this sense, different methodologies have been proposed for the determination of aldehyde [8,12,13]. The use of gas chromatography (GC) and high-performance liquid chromatography (HPLC) are the preferred techniques [14], since they allow the coupling of different detection systems and are compatible with different derivatization methodologies [15,16]. Numerous compounds have been employed in the aldehydes' derivatization, such as O-(2,3,4,5,6-pentafluorobenzyl) hydroxylamine [17], pentafluorophenylhydrazine [18], and 2,4,6-triclorophenlyhidrazine [19] for GC, as well as 4-hydrazinobenzoic acid [20], 1-naphthalenyl hydrazine [16], and N-propyl-4-hydrazine-1,8-naphthalimide [21] for HPLC. The 2,4-dinitrophenylhydrazine has been the most widely used compound [22–24]. Nonetheless, methods developed using DNPH have faced some disadvantages, such as a low selectivity, and when it is used in excess, a tendency to precipitate is shown, which limits the degree of preconcentration [25]. Furthermore, the residual presence of excess derivatizing agent can interfere with detection and instrumental separation, compromising the analytical precision and accuracy [26,27].

Different strategies have been explored to improve the derivatization process using DNPH combined with solid-phase and liquid-phase extraction steps [16,26–29]. Among these, the retention of a derivatizing agent in/on polymeric matrices stands out, as it improves stability, allows a controlled release, facilitates the derivatization process, and simultaneously reduces the amount of unreacted derivatizing agent, improving the chromatographic profile [29–31]. Materials such as polydimethylsiloxane [29], carrageenan, and chitosan [32] have been used for the derivatizing agent retention. Calcium alginate, widely used in the food, medical, and chemical industries for the immobilization of active compounds, proteins, and even microorganisms, could be an alternative to allow a gradual reagent release [33].

Therefore, this work proposes an alternative strategy for the derivatization and determination of pentanal, hexanal, heptanal, octanal, nonanal, and decanal aldehydes in edible vegetable oils, based on the encapsulation of DNPH in calcium alginate spheres, to allow a controlled release of the derivatizing agent, reducing the amount of free DNPH in the injection and improving the chromatographic profile.

2. Materials and Methods

Acetonitrile, methanol, and acetic acid were purchased from J.T. Baker (Phillipsburg, NJ, USA). Aldehydes pentanal, hexanal, heptanal, octanal, nonanal, decanal, 2-hydroxy-5-methoxybenzaldehyde, and DNPH were obtained from Sigma-Aldrich (St. Louis, MO, USA). Sodium alginate (food grade) and calcium chloride (food grade) were used. Commercial edible vegetable oil samples from soybean, canola, olive, and safflower were obtained from local supermarkets. Solutions were prepared using deionized water with a resistivity not lower than 18.0 MΩ cm, purified by a Milli-Q system (Millipore, Bedford, MA, USA). A stock solution of each aldehyde (pentanal, hexanal, heptanal, octanal, nonanal, and decanal) at a concentration of 1000 mg L^{-1} was prepared in methanol.

Chromatographic analysis was performed using an HPLC 1260 Infinity system (Agilent Technologies, Waldbronn, Germany). The system was controlled using Agilent OpenLAB CDS software (Agilent Technologies, ChemStation Edition, version A.01.05). Sep-

aration of the hydrazones was carried out using a ZORBAX Eclipse XDB-C8 column (150 × 4.6 mm, 5 µm) from Agilent Technologies. A mobile phase consisting of an aqueous solution of acetic acid at 1% *v*/*v* (A) and methanol (B) was employed using the following gradient: A/B (20/80) for 6 min, from 80 to 85% B from 6 to 9 min, 85% B from 9 to 15 min, from 85 to 80% B from 15 to 18 min, and A/B (20/80) from 18 to 20 min, at a flow rate of 1.0 mL min^{-1} and an injection volume of 20 µL. The mobile phase was filtered using a 0.45 µm membrane. Detection was performed using a diode array detector at 360 nm.

Hydrazones were characterized by infrared spectroscopy using a Perkin Elmer GX spectrometer (Waltham, MA, USA) in the range of 4000–400 cm^{-1}. Nuclear magnetic resonance (NMR) spectra at 400 MHz were obtained using a Bruker spectrometer (Bruker, Billerica, MA, USA), using $CDCl_3$ (Sigma-Aldrich) as solvent.

A solution containing sodium alginate at 2% *w*/*v* and DNPH at 1000 mg L^{-1} was prepared in a solution of deionized water and ACN at a 4:1 *v*/*v* ratio. This solution was prepared under constant stirring at 30 °C to promote the polymer dissolution. The resulting solution was dropwise added using a syringe into a calcium chloride solution at 10% *w*/*v*, remaining for 2 min. After that, the spheres were rinsed in deionized water and dried at 60 °C for 6 h. Finally, the spheres were stored in an amber flask at room temperature until their use.

Optimization of the procedure was carried out using a Taguchi $L_9(3^4)$ experimental design. The following variables were evaluated: sample volume (2, 3, and 4 mL), reaction time (60, 90, and 120 min), acetic acid concentration (86, 172, and 258 mM), and activation time (90, 120, and 150 min). Experiments were performed using mineral oil spiked with 15 mg L^{-1} of each aldehyde and 15 mg L^{-1} de 2-hydroxy-5-methoxybenzaldehyde as the internal standard. Statistical analysis was performed using Minitab 21 software, using the Σ aldehyde to internal standard area ratio as the response variable.

The representation of the derivatization methodology is shown in Figure 1. DNPH-alginate spheres were immersed in 1 mL of ACN for 120 min. Subsequently, a 2 mL aliquot of each oil was taken and doped with 15 mg L^{-1} of 2-hydroxy-5-methoxybenzaldehyde (dissolved in mineral oil) used as the internal standard. The sample was transferred to a polypropylene tube containing one DNPH-alginate sphere, and glacial acetic acid was added to achieve a concentration of 258 mM. The mixture was allowed to react for 90 min at 60 °C, 1.0 mL of ACN was added, and it was mixed and centrifuged at 2000 rpm, recovering the ACN phase. Liquid-liquid extraction was performed twice, both ACN portions were combined and evaporated under a continuous air flow, and finally the residue was reconstituted in 250 µL of methanol before its analysis by HPLC-DAD.

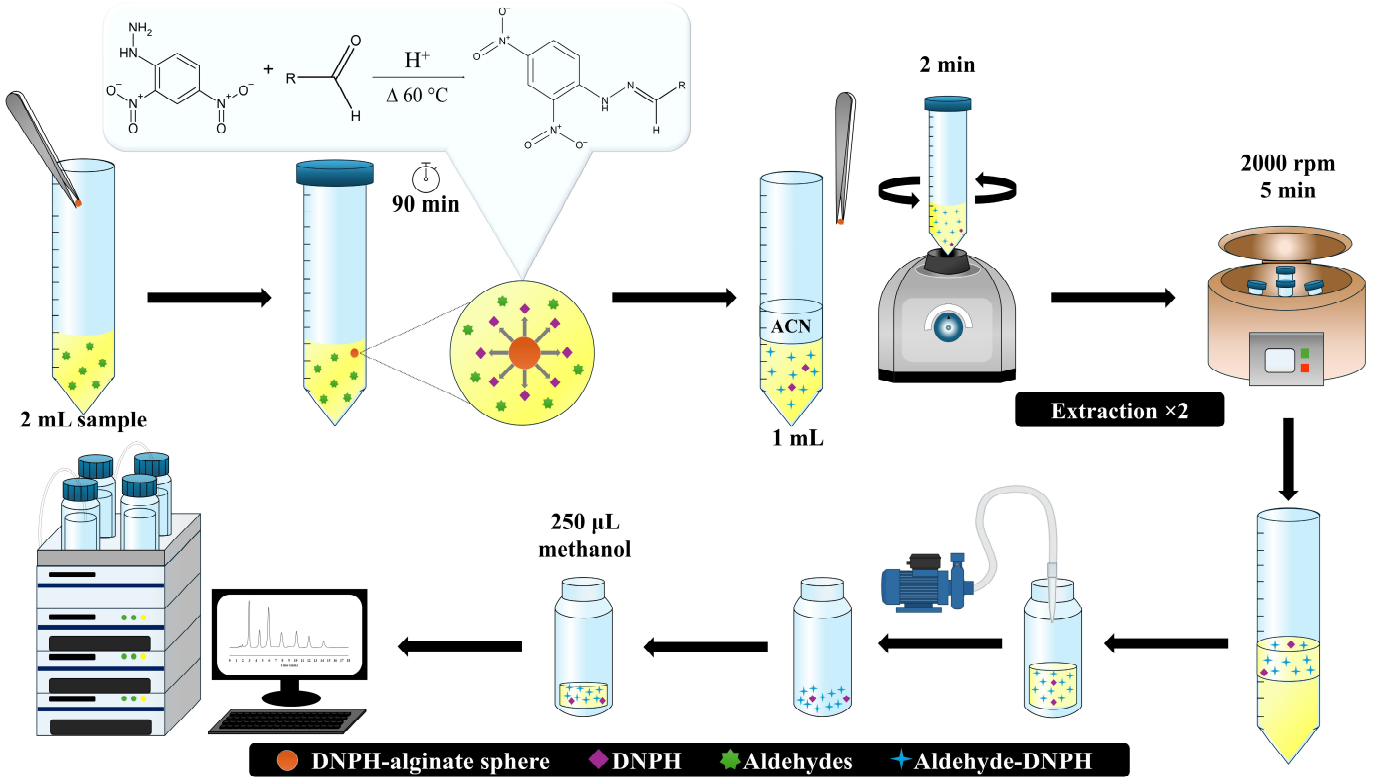

Figure 1. Schematic representation of the methodology for aldehyde determination using DNPH-alginate spheres.

3. Results and Discussion

3.1. Characterization of Alginate-DNPH Spheres

Calcium alginate spheres were prepared by ionic gelation using sodium alginate as a polymeric matrix. When DNPH-sodium alginate solution was dropwise added into a calcium chloride solution, the Ca(II) ions replaced the Na(I) ions, leading to the formation of a crosslinked three-dimensional network. The effectiveness of sphere formation was ensured by controlling alginate and calcium chloride concentrations, as well as the gelation time, resulting in homogeneous and spherical beads, which allowed for the prolonged and adequate release of the derivatizing agent.

The derivatization process using the spheres was evaluated using two strategies: (1) hydrated spheres (after their formation in the calcium chloride solution) and (2) spheres that were dried at 60 °C for 4 h. Figure S1a shows a bead in its hydrated state with a spherical shape, with an average diameter of 0.54 ± 0.03 mm, while the sphere obtained after the drying process presented an irregular shape and an average diameter of 0.19 ± 0.02 cm (Figure S1b).

The release of DNPH from both spheres was compared, showing that the dried spheres allowed a more controlled release of the derivatizing agent. Furthermore, the dried DNPH-calcium alginate spheres were stable in edible oils, and the hydrazones formed were solubilized in the oil phase allowing the liquid-liquid extraction with ACN. The calcium alginate phase remained stable, and therefore the viscosity was not affected. In contrast, the non-dried spheres tended to break, releasing the DNPH and water contained inside them, which negatively affected the derivatization reaction. Therefore, the dried spheres were selected for the experiment design.

The infrared spectra obtained for sodium alginate, DNPH, and alginate-DNPH spheres are presented in Figure S2. FTIR spectrum of sodium alginate (Figure S2a) showed a characteristic band around 3250 cm^{-1} corresponding to the stretching vibration of -OH groups,

bands at 1600 cm^{-1} and 1400 cm^{-1} corresponding to the asymmetric and symmetric stretching vibrations of the carboxylate group [34], and a band at 1000 cm^{-1}, attributed to C-O-C stretching vibrations [35]. Meanwhile, the DNPH spectrum (Figure S2b) showed a band at 3330 cm^{-1} corresponding to N-H stretching of the hydrazine group, signals in the 3000–3100 cm^{-1} intervals associated with C-H stretching, a band at 1600 cm^{-1} attributed to C=C stretching vibration of the aromatic ring, and bands around 1500–1300 cm^{-1}, characteristic of the asymmetric and symmetric stretching vibrations of NO_2 groups [36,37]. The DNPH-alginate spectrum (Figure S2c) showed representative bands of both the polysaccharide and DNPH, highlighting the presence of the band at 3330 cm^{-1} corresponding to N-H stretching and signals in the 3090–3110 cm^{-1} interval, characteristic of aromatic C-H stretching. The FTIR of alginate-DNPH sphere confirmed the preservation of the characteristic absorption bands of both components, without the appearance of new bands indicative of covalent bond formation. The spectral variations could be attributed to weak interactions such as hydrogen interaction or van der Waals forces. The spectral similarity supported the absence of chemical modification of DNPH in the alginate matrix. Additionally, the effective release of DNPH from the alginate spheres and the subsequent formation of aldehyde-DNPH hydrazones confirmed that the interactions inside the structure were non-covalent.

3.2. Characterization of Aldehyde-DNPH

To obtain the corresponding hydrazones between DNPH and the fatty aldehydes pentanal, hexanal, heptanal, octanal, nonanal, and decanal, 5 mL ACN containing 1000 mg L^{-1} of DNPH was placed with the respective aldehyde in excess for 90 min. After the reaction time, the solvent and the excess aldehyde were evaporated until a powder was obtained.

The hydrazones were characterized by FTIR spectroscopy. Figure S3b corresponds to the spectrum of hexanal, which showed bands around 3000–2900 cm^{-1} corresponding to the symmetric and asymmetric stretching vibrations of methylene and methyl groups of the aliphatic chain. In the 2800–2600 cm^{-1} interval, bands corresponding to the O=C-H bond of the aldehyde (Fermi resonance) were observed, while at 1717 cm^{-1}, the characteristic stretching vibration band of the aldehyde C=O group was visible, and at 1400 cm^{-1}, the C-H bending vibration band appeared [38–40]. The analyzed aldehydes showed only changes in the length of the aliphatic chain, exhibiting a similar profile in the FTIR spectra.

In the FTIR spectrum of the hexanal-DNPH hydrazone (Figure S3c), a shift and increase in intensity of the signal at 3295 cm^{-1} corresponding to the N-H stretching vibration was noticed. Also, bands at 3000–2900 cm^{-1} corresponding to the symmetric and asymmetric stretching vibrations of methylene and methyl groups of the aliphatic chain and the appearance of a band in the 1600–1500 cm^{-1} range corresponding to C=N stretching were observed. Meanwhile, the vibration bands corresponding to the aldehyde OC-H bond and the C=O stretching vibration (2800–2600 cm^{-1} and 1717 cm^{-1} respectively) disappeared compared to the starting materials, indicating the hydrazone formation. All hydrazones showed only changes in the length of the aliphatic chain, exhibiting a similar profile in the obtained FTIR spectra [41].

Additionally, ^{1}H NMR spectra allowed the structural analysis of the reagents (DNPH and aldehydes) and the obtained hydrazones. For hexanal ^{1}H NMR: ($CDCl_3$, T = 25 °C) δ ppm: 9.75 (s, -CHO, 1H), 2.40 (m, -$OHCCH_2$, 2H), 1.62 (m, -CH_2, 2H), 1.30 (m, -CH_2, 4H) 0.89 (t, -CH_3, 3H). For DNPH ^{1}H NMR ($CDCl_3$, T = 25 °C) δ ppm: 9.44 (s, -NH-N, 1H) 9.10 (d, DNPH aromatic protons, 1H), 8.29 (d, DNPH aromatic protons, 1H), 7.84 (d, DNPH aromatic protons, 1H), 3.99 (s, -NH, 2H). For hexanal-DNPH ^{1}H NMR: ($CDCl_3$, T = 25 °C) δ ppm: 11.03 (s-NH-N, 1H), 9.15 (d, DNPH aromatic protons, 1H), 8.31 (d, DNPH aromatic

protons, 1H), 7.94 (d, DNPH aromatic protons, 1H) 7.55 (t-CHN, 1H), 2.44 (m, -NHCCH$_2$, 2H), 1.66 (m, -CH$_2$, 2H), 1.40 (m, -CH$_2$, 4H) 0.95 (t, -CH$_3$, 3H). Figure S4 shows the spectra of hexanal, DNPH, and the corresponding hexanal-DNPH hydrazone. Comparing the spectra, when the hydrazones were formed, the aldehyde signal, a characteristic shift of approximately 9.7 ppm, disappeared [42]. However, the signals corresponding to the aliphatic chain and the aromatic ring of DNPH were observed [43]. In addition, a signal associated with the H-C=N group was visible around 7.55 ppm, while the NH proton showed a chemical shift to 11.03 ppm [37]. These signals confirmed the formation of the respective hydrazone. The spectra of the other hydrazones formed are shown in Figure S5, exhibiting the following shifts in the signals:

For pentanal-DNPH ^{1}H NMR: (CDCl$_3$, T = 25 °C) δ ppm: 11.07 (s-NH-N, 1H), 9.13 (d, DNPH aromatic protons, 1H), 8.33 (d, DNPH aromatic protons, 1H), 7.92 (d, DNPH aromatic protons, 1H) 7.52 (t-CHN, 1H), 2.43 (m, -NHCCH$_2$, 2H), 1.59 (m, -CH$_2$, 2H), 1.33 (m, -CH$_2$, 2H) 0.94 (t, -CH$_3$, 3H). For heptanal-DNPH ^{1}H NMR: (CDCl$_3$, T = 25 °C) δ ppm: 11.00 (s-NH-N, 1H), 9.11 (d, DNPH aromatic protons, 1H), 8.27 (d, DNPH aromatic protons, 1H), 7.90 (d, DNPH aromatic protons, 1H) 7.52 (t-CHN, 1H), 2.39 (m, -NHCCH$_2$, 2H), 1.55 (m, -CH$_2$, 2H), 1.31 (m, -CH$_2$, 6H) 0.89 (t, -CH$_3$, 3H). For octanal-DNPH ^{1}H NMR: (CDCl$_3$, T = 25 °C) δ ppm: 10.98 (s-NH-N, 1H), 9.07 (d, DNPH aromatic protons, 1H), 8.24 (d, DNPH aromatic protons, 1H), 7.88 (d, DNPH aromatic protons, 1H) 7.51 (t-CHN, 1H), 2.38 (m, -NHCCH$_2$, 2H), 1.57 (m, -CH$_2$, 2H), 1.26 (m, -CH$_2$, 8H) 0.85 (t, -CH$_3$, 3H). For nonanal-DNPH ^{1}H NMR: (CDCl$_3$, T = 25 °C) δ ppm: 10.95 (s-NH-N, 1H), 9.05 (d, DNPH aromatic protons, 1H), 8.21 (d, DNPH aromatic protons, 1H), 7.85 (d, DNPH aromatic protons, 1H) 7.47 (t-CHN, 1H), 2.35 (m, -NHCCH$_2$, 2H), 1.57 (m, -CH$_2$, 2H), 1.21 (m, -CH$_2$, 10H) 0.82 (t, -CH$_3$, 3H). For decanal-DNPH ^{1}H NMR: (CDCl$_3$, T = 25 °C) δ ppm: 10.95 (s-NH-N, 1H), 9.04 (d, DNPH aromatic protons, 1H), 8.21 (d, DNPH aromatic protons, 1H), 7.85 (d, DNPH aromatic protons, 1H) 7.47 (t-CHN, 1H), 2.35 (m, -NHCCH$_2$, 2H), 1.58 (m, -CH$_2$, 2H), 1.24 (m, -CH$_2$, 12H) 0.81 (t, -CH$_3$, 3H).

3.3. Optimization of Reaction Conditions

The derivatization with DNPH applied in the aldehyde determination is based on the hydrazone synthesis through a condensation reaction influenced by diverse variables, such as sample volume, reaction time, acid concentration, and activation time. Therefore, optimization was carried out using a Taguchi L$_9$(3^4) experiment design where the intervals for each variable were defined based on a prior evaluation of the selected intervals [9,44], generating the orthogonal matrix of the Taguchi experimental design shown in Table 1. Each experiment was performed in a doped mineral for method optimization and validation due to its stability against oxidation because of its high saturated hydrocarbon content, which allows a clear evaluation of the effect of the studied variables. For the analysis, a sphere was used that contains an estimated concentration of 0.06 ± 0.01 mg of DNPH.

Table 1. Taguchi orthogonal array L$_9$(3^4).

Exp	Sample Volume (mL)	Reaction Time (min)	Activation Time (min)	[AcOH] (mM)	∑ (RCHOs/IS)
1	2	60	90	86	1.31
2	2	90	120	172	1.41
3	2	120	150	258	1.51
4	3	60	150	86	1.17
5	3	90	90	172	0.90
6	3	120	120	258	1.10
7	4	60	120	86	0.58
8	4	90	150	172	0.70
9	4	120	90	258	0.68

Multiple aliphatic, α, β-unsaturated aldehydes, and hydroxyaldehydes generated from lipid oxidation have been described [10], so 2-hydroxy-5-methoxybenzaldehyde was selected as an internal standard since it is not an aldehyde usually described in the analytical matrix or generated from lipid oxidation. Although this aldehyde is structurally different from the evaluated ones, no interference was observed in the formation of the corresponding hydrazone, making it suitable for the monitoring of the technique. The optimization of derivatization conditions using the Taguchi design allowed identification of the levels of each variable, which offered the highest analytical response in terms of the ΣAldehyde-to-IS peak area ratio. According to the results (Figure 2), a sample volume of 2.0 mL was the value of the variable with the greatest contribution among the evaluated factors. On the other hand, increasing the oil volume provoked a decrease on the response variable related to the equilibrium in mass transfer governed by the dependence between sample volume and extractant volume, as the distribution decreases with increasing sample volume [45,46]. The highest acetic acid concentration (258 mM) also favored an increase in the response signal, since the hydrazone formation occurs through a nucleophilic addition to the carbonyl group followed by a dehydration step. However, the addition of an acidic medium is required to protonate the oxygen and enable nucleophilic addition, with this step being crucial [47]. Finally, sphere conditioning time showed an improvement in derivatization capacity when longer activation periods were employed. This increase in analytical response can be attributed to structural changes in the alginate matrix that modifies DNPH availability. After spheres dry, porosity decreases, and the polymer network becomes denser, limiting internal diffusion of the encapsulated compound. However, the immersion in ACN reduces the polymer rigidity and improves internal mobility, facilitating the diffusion of the derivatizing reagent. Thus, a longer conditioning period facilitates DNPH diffusion toward the sphere surface [48–51]. Related to the reaction time variable, results indicated that this factor influenced the process performance, since sufficient reaction time is required for its completion. In short times, the reaction cannot go on quantitatively, whereas excessively long reaction times could lead to the formation of other species or product decomposition. The optimal values obtained from the experiment design were a sample volume of 2.0 mL, [acetic acid] of 258 mM, 150 min of sphere activation, and 90 min of reaction. These conditions were used for subsequent experiments.

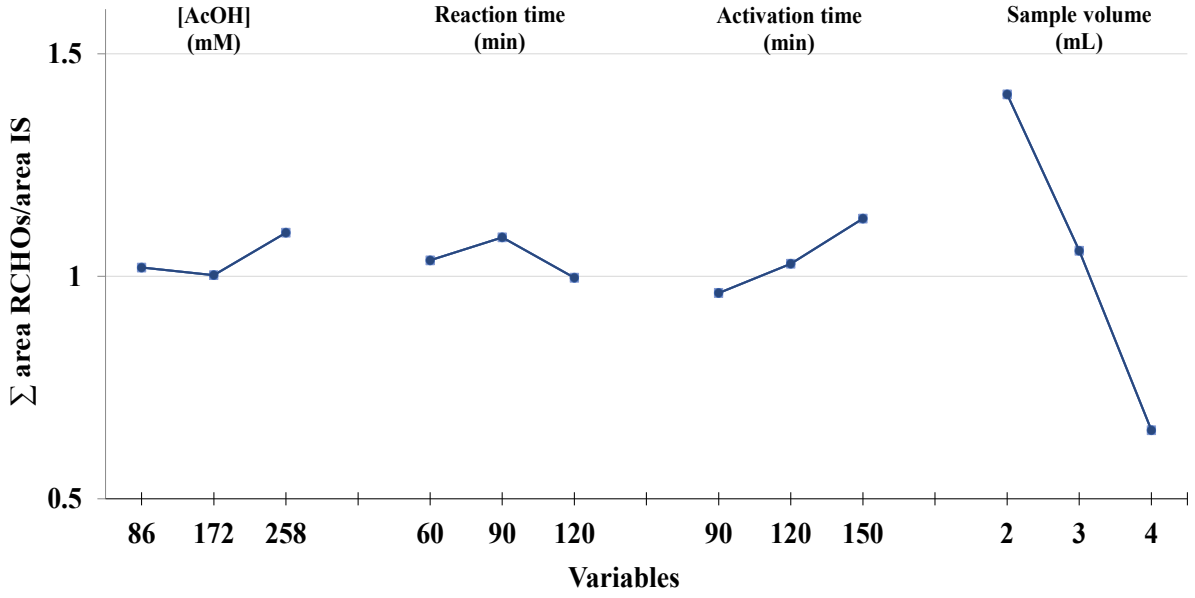

Figure 2. Main effect plot for mean of Taguchi design.

Under optimal conditions, the calibration curves were constructed, obtaining linear intervals from 2.34 to 50.0 mg L^{-1}. Analytical parameters are presented in Table 2. The limits of detection (LOD) ranged from 0.77 to 1.41 mg L^{-1}, calculated at a signal-to-noise ratio of 3.29, and the limits of quantification (LOQ) ranged from 2.34 to 4.28 mg L^{-1}, calculated at a signal-to-noise ratio of 10, according to IUPAC criteria. It has been reported that aldehyde concentrations above 40 mg L^{-1} generate perceptible rancid odors and flavors in foods, whereas levels below 5 mg L^{-1} do not modify the sensory profile [52], indicating that the achieved LODs allow the aldehyde detection within a relevant range to evaluate oxidative spoilage.

Table 2. Regression parameters of the calibration curves for the aldehydes.

Aldehyde	r^2	$b_1 \pm \delta b_1$	$b_0 \pm \delta b_0$	LOD (mg L^{-1})	LOQ (mg L^{-1})
Pentanal	0.999	0.391 ± 0.017	0.001 ± 0.035	1.34	4.07
Hexanal	0.999	0.949 ± 0.034	0.118 ± 0.058	1.09	3.30
Heptanal	0.999	0.362 ± 0.020	0.036 ± 0.039	1.41	4.28
Octanal	0.999	0.314 ± 0.009	0.064 ± 0.016	0.77	2.34
Nonanal	0.999	0.191 ± 0.006	0.055 ± 0.013	0.82	2.51
Decanal	0.999	0.116 ± 0.003	0.037 ± 0.006	0.79	2.40

The method precision was estimated as repeatability and reproducibility in terms of relative standard deviation (% RSD, n = 3) at three concentration levels (20, 30, and 40 mg L^{-1}) (Table 3). The repeatability and reproducibility values were below 10% in all cases, indicating adequate precision. The method accuracy was evaluated by recovery assays at three concentration levels (25, 35, and 45 mg L^{-1}). In this case, the results ranged from 91.18 to 109.34%, with %RSD values below 10% at all evaluated levels. These results indicate that the proposed methodology for aldehyde determination is adequate in terms of precision and accuracy.

Table 3. Repeatability, reproducibility, and recovery values at different concentration levels.

Aldehyde	Repeatability (%RSD, n = 3)			Reproducibility (%RSD, n = 3)			% Recovery (%RSD, n = 3)		
	20 mg L^{-1}	30 mg L^{-1}	40 mg L^{-1}	20 mg L^{-1}	30 mg L^{-1}	40 mg L^{-1}	25 mg L^{-1}	35 mg L^{-1}	45 mg L^{-1}
Pentanal	3.40	3.75	4.92	7.61	5.79	3.80	91.18 (7.22)	102.24 (7.93)	96.79 (4.72)
Hexanal	4.22	3.91	5.18	7.45	4.01	5.18	92.15 (9.66)	97.84 (8.20)	99.02 (5.98)
Heptanal	3.18	3.36	5.22	7.60	6.18	4.07	93.33 (8.16)	109.34 (7.76)	100.65 (8.86)
Octanal	3.58	3.14	6.73	8.13	4.89	3.81	93.35 (9.64)	108.75 (8.40)	104.46 (8.23)
Nonanal	3.65	2.53	5.63	4.85	6.89	9.42	98.21 (8.85)	109.34 (7.42)	106.14 (7.66)
Decanal	1.36	2.56	4.84	6.63	5.47	6.96	101.43 (3.88)	108.51 (4.60)	103.60 (6.02)

The aldehyde content was determined in four fresh edible vegetable oils subjected to a thermal oxidation process by continuously heating at 100 °C for 7 days. Under these conditions, safflower oil exhibited the highest degradation, with quantifiable concentrations of the six aldehydes evaluated (Figure 3), whereas soybean and canola oils showed lower concentrations and no detection of decanal. In safflower oil, nonanal was the predominant aldehyde, followed by hexanal, which can be attributed to the high proportion of oleic and linoleic acids, respectively, whose oxidative degradation favors the formation of these

compounds. This behavior is consistent with the fatty acid profile reported in the literature, where oleic and linoleic acids account for approximately 93.27% of the total fatty acids. Similarly, in canola and soybean oils, where hexanal and nonanal were the predominant, respectively, oleic and linoleic acids represent approximately 77.04% of the total fatty acids in canola oil and 86.02% in soybean oil [16,53]. On the contrary, olive oil showed the lowest aldehyde formation among the samples studied, possibly due to the added natural antioxidant compounds, such as phenols and tocopherols, which can delay oxidative degradation [54].

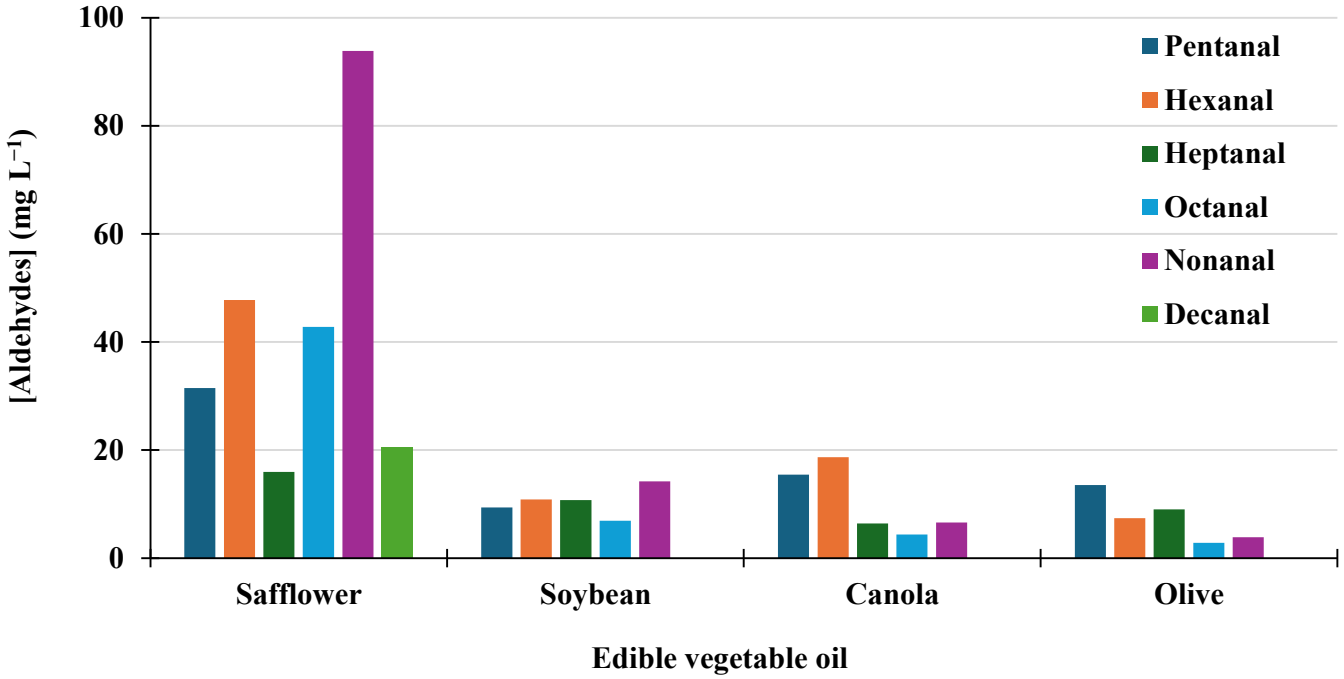

Figure 3. Concentrations of aldehydes in edible vegetable oils after thermal oxidation.

Conventional methodologies for aldehyde derivatization using DNPH are based on the direct addition of the derivatizing agent and the use of high concentrations compared to aldehydes to ensure a complete reaction. However, this excess can provoke interference in the chromatographic profiles. The proposed methodology represents an advantage because the use of DNPH encapsulated in alginate allows the gradual release of the reagent and reduces the presence of unreacted DNPH in the injection. This behavior is reflected in the chromatograms of the blank (Figure 4a) and the enriched mineral oil standard (Figure 4b), where the signal corresponding to free derivatizing agent is not observed. Likewise, the chromatogram of the sample subjected to thermal oxidation (Figure 4c) besides the six aldehydes evaluated multiple peaks at shorter retention times were observed, not appreciated in the blank or in the standard samples. This suggests that the derivatization of other carbonyl compounds could be resolved in the absence of interferences caused by excess of DNPH (Figure S6). These results indicate that the proposed methodology has potential to broaden its application to oxidation products other than those analyzed in this study and to obtain more comprehensive lipid degradation profiles in complex matrices.

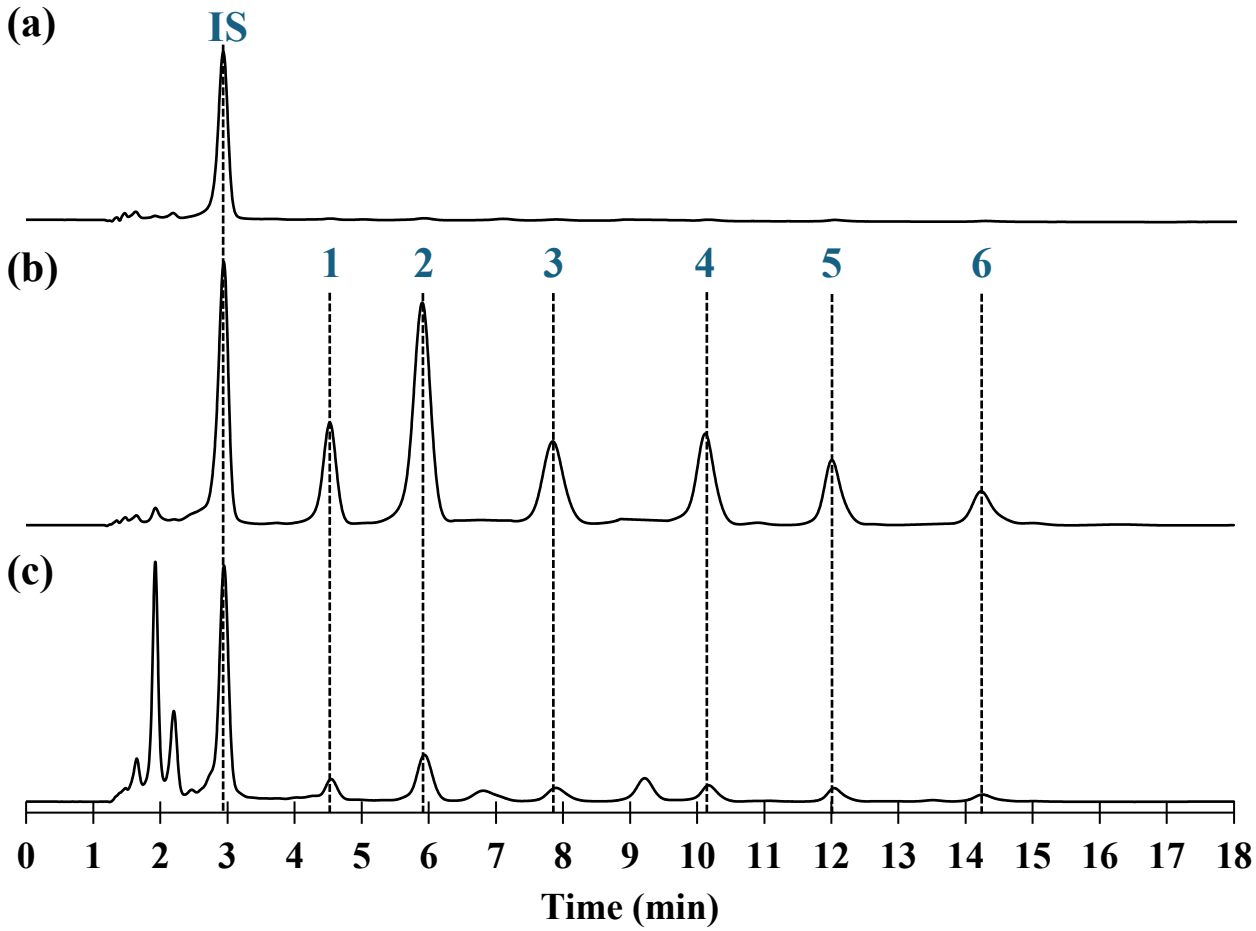

Figure 4. Chromatograms of (**a**) blank (**b**) mineral oil enriched with 40 mg L^{-1} of each aldehyde (**c**) safflower oil sample heated to 100 °C for 7 days. Peak assignments: IS: internal standard 15 mg L^{-1}, 1: pentanal, 2: hexanal, 3: heptanal, 4: octanal, 5: nonanal, 6: decanal.

Generally, other conventional methodologies described in the literature (Table 4) present different limitations. For example, some of them employ derivatizing agents that require complex synthesis [55], or they use solid-phase extraction protocols that require extensive adsorbent preparation [56]. In contrast, the proposed based on DNPH-alginate spheres allows direct derivatization inside the sample matrix, reducing sample handling. Furthermore, the preparation of the spheres is quite simple and not expensive. Additionally, different studies determining comparable aldehyde concentrations in oxidized edible vegetable oil samples confirm that extremely low LODs are not required for lipid oxidation assessment [11,57]. In this sense, a DAD detection system should be enough compared to a system coupled to mass spectrometry, which would exceed the analytical requirements of these oil samples.

Table 4. Comparative table of analytical methodologies reported for aldehyde determination.

Aldehydes	Methodology	Sample Treatment	Reagent	Analytical Method	LOD	REF
Malondialdehyde, 4-hydroxy-2-hexenal, 4-hydroxy-2-nonenal, 2,4-decadienal	LLE followed by derivatization	LLE	DNPH	LC-MS/MS	0.02–0.14 mg kg^{-1}	[11]
4-Hydroxy-nonenal	LLE followed by derivatization	LLE	Pentafluorophenylhydrazine	UHPLC-MS/MS	10.9 nM	[58]

Table 4. *Cont.*

Aldehydes	Methodology	Sample Treatment	Reagent	Analytical Method	LOD	REF
Hexanal and Heptanal	Synthesized levofloxacin-hydrazide-based mass tags (LHMTs) combined with dummy magnetic molecularly imprinted polymers.	Magnetic dispersive solid-phase extraction using dummy molecularly imprinted polymers (DMMIPs)	Levofloxacin-hydrazide-based mass tags (LHMTs, laboratory-synthesized)	UHPLC–MS/MS	0.5 pM	[55]
Formaldehyde, acetaldehyde, propanal, butanal, pentanal, hexanal, heptanal	Micro solid-phase extraction using a custom-prepared cyclodextrin-based polymer sorbent	µ-SPE-D	DNPH	µ-SPE-D-HPLC.	0.024–2.5 µg L^{-1}	[56]
Hexanal and heptanal	DNPH adsorbed onto the surface of magnetite/silica/poly(methacrylic acid-co-ethylene glycol dimethacrylate) ($Fe_3O_4/SiO_2/P$(MAA-co-EGDMA	Magnetic solid-phase extraction coupled with in situ derivatization (MSPE-ISD)	DNPH	MSPE-ISD-HPLC-UV	1.7–2.5 nmol L^{-1}	[28]
4-hydroxy-2-nonenal, 2,4-decadienal, 2,4-heptadienal, 4-hydroxy-2-hexenal, acrolein, 2-heptenal, 2-octenal, 4,5-epoxy-2decadal, 2-decenal, and 2-undecenal.	LLE followed by derivatization	LLE	DNPH	UFLC-DAD-ESI-MS	0.03–0.1 mg L^{-1}	[59]
trans-2-butenal, trans-2-pentenal, trans-2-hexenal, trans-2-heptenal, trans-2-octenal, trans-2-nonenal, trans-2-decenal and trans-2-undecenal		LLE	2-hydrazinopyridine and 2-hydrazino-5-methylpyridine	DCBI-MS/MS	0.03–0.18 mg L^{-1}	[57]
Pentanal, hexanal, heptanal, octanal, nonanal and decanal	DNPH-alginate sphere-based derivatization	LLE	DNPH	HPLC-DAD	0.77–1.41 mg L^{-1}	This work

4. Conclusions

A methodology was developed for the derivatization and determination of six saturated fatty aldehydes in oxidized vegetable edible oils using DNPH encapsulated in calcium alginate spheres. The gradual release of the derivatizing agent allowed the acquisition of cleaner chromatographic profiles, highlighting the absence of the chromatographic signal corresponding to unreacted DNPH in the blank sample and in the spiked standard. This confirms its adequate interaction with the analytes for their separation and detection by HPLC-DAD, with limits of detection from 0.77 to 1.41 mg L^{-1}, suitable to follow oxidative degradation in fatty foods. Furthermore, the absence of interferences derived from free DNPH, far from being limited exclusively to the aldehydes analyzed in this study, could allow the evaluation of other lower molecular aldehydes.

Supplementary Materials: The following supporting information can be downloaded at https://www.mdpi.com/article/10.3390/separations13020075/s1. Figure S1. DNPH-alginate spheres (a) hydrated form (b) after drying process; Figure S2. FTIR spectra of (a) sodium alginate (b) DNPH (c)

DNPH-alginate; Figure S3. FTIR spectra of (a) DNPH (b) hexanal (c) hexanal dinitrophenylhydrazone; Figure S4. 1H NMR spectra of (a) hexanal (b) DNPH (c) hexanal-DNPH; Figure S5. 1H NMR spectra of (a) pentanal-DNPH (b) heptanal-DNPH (c) octanal-DNPH (d) nonanal-DNPH (e) decanal-DNPH; Figure S6. Chromatograms of (a) derivatization of aldehydes using DNPH in solution (b) derivatization of aldehydes using DNPH encapsulated in calcium alginate spheres.

Author Contributions: Conceptualization, J.A.R.; methodology, F.E.S.-M.; validation, J.L.-T. and F.E.S.-M.; formal analysis, E.M.S. and F.E.S.-M.; investigation, F.E.S.-M. and A.C.M.-P.; resources, J.A.R.; data curation, J.L.-T. and A.C.M.-P.; writing-original draft preparation, F.E.S.-M. and E.M.S.; writing—review and editing, J.L.-T. and J.A.R.; visualization, F.E.S.-M. and E.M.S.; supervision, A.C.M.-P. and J.A.R. All authors have read and agreed to the published version of the manuscript.

Funding: This research received no external funding.

Data Availability Statement: The authors confirm that the data supporting the findings of this study are available within the article.

Acknowledgments: The authors thank the financial support from Secretaria de Ciencia, Humanidades, Tecnologia e Innovacion (SECIHTI) (SNI distinction as research membership, scholarship and program "Ayudante de investigador SNI").

Conflicts of Interest: The authors declare no conflicts of interest.

Abbreviations

The following abbreviations are used in this manuscript:

ACN	Acetonitrile
AcOH	Acetic acid
DCBI-MS/MS	Desorption Corona Beam Ionization tandem mass spectrometry
DMMIPs	Dual-template magnetic molecularly imprinted polymers
DNPH	2,4-dinitrophenylhydrazine
Exp	Experiment
Fe_3O_4/SiO_2/P(MAA-co-EGDMA	Magnetite/silica/poly(methacrylic acid-co-ethylene glycol dimethacrylate)
FTIR	Fourier transform infrared spectroscopy
GC	Gas chromatography
HPLC	High-performance liquid chromatography
HPLC-DAD	High-performance liquid chromatography with diode-array detection
HPLC-UV	High-performance liquid chromatography with ultra-violet detection
IS	Internal standard
LC-MS/MS	Liquid chromatography with tandem mass spectrometry
LHMTs	Levofloxacin-hydrazide-based mass tags
LLE	Liquid-liquid extraction
LOD	Limit of detection
LOQ	Limit of quantification
MSPE-ISD	Magnetic solid phase extraction coupled with in situ derivatization
NMR	Nuclear magnetic resonance
REF	Reference
RSD	Relative standard deviation
UHPLC-MS/MS	Ultra-high performance liquid chromatography-mass spectrometry/mass spectrometry
UFLC-DAD-ESI-MS	Ultra-Fast liquid chromatography coupled with diode array and electrospray ionization mass spectrometry
μ-SPE-D	Micro solid-phase extraction and derivatization

References

1. Nieto, G.; Lorenzo, J.M. Plant source: Vegetable oils. In *Food Lipids*; Academic Press: Cambridge, UK, 2022; pp. 69–85. [CrossRef]

2. Zhang, W.; Zhu, H.; Xie, W.; Du, C.; Fang, X.; Zhang, R.; Lin, Y. Highly sensitive analysis of fatty aldehydes in vegetable oils using a novel coumarin-based fluorescent probe by HPLC for quality control. *Microchem. J.* **2024**, *205*, 111180. [CrossRef]
3. Wang, L.; Wang, J.; Xu, J.; Liu, S.; Huang, S.; Han, S.; Lv, M. Highly sensitive qualitative and quantitative detection of saturated fatty aldehydes in edible vegetable oils using a "turn-on" fluorescent probe by high-performance liquid chromatography. *J. Chromatogr. A* **2020**, *1621*, 461063. [CrossRef]
4. Suh, J.H.; Niu, Y.S.; Hung, W.L.; Ho, C.T.; Wang, Y. Lipidomic analysis for carbonyl species derived from fish oil using liquid chromatography–tandem mass spectrometry. *Talanta* **2017**, *168*, 31–42. [CrossRef] [PubMed]
5. Zhang, D.C.; Liu, J.J.; Jia, L.Z.; Wang, P.; Han, X. Speciation of VOCs in the cooking fumes from five edible oils and their corresponding health risk assessments. *Atmos. Environ.* **2019**, *211*, 6–17. [CrossRef]
6. Guo, X.Y.; Cheng, L.Y.; Chang, C.; Jiang, X.M.; Gao, P.; Zhong, W.; Yin, J. Toxic aldehydes in fried foods: Formation, analysis, and reduction strategies. *Food Control* **2025**, *169*, 110993. [CrossRef]
7. Cao, G.; Ruan, D.; Chen, Z.; Hong, Y.; Cai, Z. Recent developments and applications of mass spectrometry for the quality and safety assessment of cooking oil. *TrAC Trends Anal. Chem.* **2017**, *96*, 201–211. [CrossRef]
8. Zhao, M.; Liu, Z.; Zhang, W.; Xia, G.; Li, C.; Rakariyatham, K.; Zhou, D. Advance in aldehydes derived from lipid oxidation: A review of the formation mechanism, attributable food thermal processing technology, analytical method and toxicological effect. *Food Res. Int.* **2025**, *203*, 115811. [CrossRef]
9. Custodio-Mendoza, J.A.; Aja-Macaya, J.; Valente, I.M.; Rodrigues, J.A.; Almeida, P.J.; Lorenzo, R.A.; Carro, A.M. Determination of malondialdehyde, acrolein and four other products of lipid peroxidation in edible oils by gas-diffusion microextraction combined with dispersive liquid–liquid microextraction. *J. Chromatogr. A* **2020**, *1627*, 461397. [CrossRef] [PubMed]
10. Huang, J.; Zhao, N.; Wang, L.; He, H.; Song, Z.; Wang, X. Effect of amino acids on the formation and distribution of volatile aldehydes in high-oleic sunflower oil during frying. *Food Res. Int.* **2024**, *192*, 114749. [CrossRef]
11. Douny, C.; Tihon, A.; Bayonnet, P.; Brose, F.; Degand, G.; Rozet, E.; Scippo, M.L. Validation of the analytical procedure for the determination of malondialdehyde and three other aldehydes in vegetable oil using liquid chromatography–tandem mass spectrometry and application to linseed oil. *Food Anal. Methods* **2015**, *8*, 1425–1435. [CrossRef]
12. Ramírez-Montes, S.; Santos, E.M.; Galán-Vidal, C.A.; Tavizon-Pozos, J.A.; Rodriguez, J.A. Classification of edible vegetable oil degradation using multivariate data analysis from electrochemical techniques. *Food Anal. Methods* **2021**, *14*, 2597–2606. [CrossRef]
13. Sukharev, S.; Mariychuk, R.; Onysko, M.; Sukhareva, O.; Delegan-Kokaiko, S. Fast determination of total aldehydes in rainwaters in the presence of interfering compounds. *Environ. Chem. Lett.* **2019**, *17*, 1405–1411. [CrossRef]
14. El-Maghrabey, M.H.; Hashem, H.M.; El Hamd, M.A.; El-Shaheny, R.; Kishikawa, N.; Kuroda, N.; Magdy, G. Comprehensive greenness evaluation of reported chromatographic methods for aldehydes determination as clinical biomarkers and food quality indicators. *TrAC Trends Anal. Chem.* **2024**, *171*, 117548. [CrossRef]
15. Kishikawa, N.; El-Maghrabey, M.H.; Kuroda, N. Chromatographic methods and sample pretreatment techniques for aldehydes determination in biological, food, and environmental samples. *J. Pharm. Biomed. Anal.* **2019**, *175*, 112782. [CrossRef]
16. Lopez-Tellez, J.; Ibarra, I.S.; Santos, E.M.; Mondragon-Portocarrero, A.C.; Rodriguez, J.A. Aldehydes determination in edible oil samples employing 1-naphthalenyl hydrazine as derivatizing agent followed by HPLC-FLD. *Microchem. J.* **2025**, *213*, 113658. [CrossRef]
17. Filipowska, W.; Jaskula-Goiris, B.; Ditrych, M.; Schlich, J.; De Rouck, G.; Aerts, G.; De Cooman, L. Determination of optimal sample preparation for aldehyde extraction from pale malts and their quantification via headspace solid-phase microextraction followed by gas chromatography–mass spectrometry. *J. Chromatogr. A* **2020**, *1612*, 460647. [CrossRef]
18. Wang, Q.; O'Reilly, J.; Pawliszyn, J. Determination of low-molecular-mass aldehydes by automated headspace solid-phase microextraction with in-fiber derivatization. *J. Chromatogr. A* **2005**, *1071*, 147–154. [CrossRef]
19. Castejón-Musulén, O.; Aragón-Capone, A.M.; Ontañón, I.; Peña, C.; Ferreira, V.; Bueno, M. Accurate quantitative determination of the total amounts of Strecker aldehydes contained in wine. Assessment of their presence in table wines. *Food Res. Int.* **2022**, *162*, 112125. [CrossRef] [PubMed]
20. de Lima, L.F.; Brandão, P.F.; Donegatti, T.A.; Ramos, R.M.; Gonçalves, L.M.; Cardoso, A.A.; Rodrigues, J.A. 4-Hydrazinobenzoic acid as a derivatizing agent for aldehyde analysis by HPLC-UV and CE–DAD. *Talanta* **2018**, *187*, 113–119. [CrossRef]
21. Chen, L.; Fu, Y.J.; Fang, W.L.; Guo, X.F.; Wang, H. Screening of a highly effective fluorescent derivatization reagent for carbonyl compounds and its application in HPLC with fluorescence detection. *Talanta* **2018**, *186*, 221–228. [CrossRef]
22. Elbanna, A.G.; Ahmed, H.M.; Barseem, A.; Farag, A.S. An innovative voltammetric determination of bempedoic acid: Evaluating analytical green metrics. *Microchem. J.* **2025**, *218*, 115402. [CrossRef]
23. Wang, S.Y.; Liu, H.; Zhu, J.H.; Zhou, S.S.; Xu, J.D.; Zhou, J.; Zhu, H. 2,4-Dinitrophenylhydrazine capturing combined with mass defect filtering strategy to identify aliphatic aldehydes in biological samples. *J. Chromatogr. A* **2022**, *1679*, 463405. [CrossRef] [PubMed]
24. Perera, H.; Lebanov, L.; Rodriguez, E.S.; Taoum, A.; Paull, B.; Sivret, E. Analytical approaches for sampling and assessing volatile organic compounds emitted from engineered wood products. *Build. Environ.* **2025**, *271*, 112578. [CrossRef]

25. Zhang, Y.; Shang, X.; Guo, J.; Ao, L.; Shen, C.; Liu, M.; Deng, B. A computationally driven screening–construction–mechanism strategy of magnetic molecularly imprinted polymers for aliphatic aldehydes detection. *Food Chem.* **2025**, *496*, 146974. [CrossRef] [PubMed]
26. Temerdashev, A.; Atapattu, S.N.; Feng, Y.Q. A tutorial on solid-phase analytical derivatization in sample preparation applications. *J. Chromatogr. Open* **2024**, *6*, 100157. [CrossRef]
27. Peng, S.; Wen, Y.; Ming, Y.; Huang, T.; Xu, G.; Yan, J.; Li, J. Molecularly imprinted polymer based enrichment and separation for trace analysis in capillary electrophoresis. *Talanta* **2026**, *297*, 128549. [CrossRef]
28. Liu, J.F.; Yuan, B.F.; Feng, Y.Q. Determination of hexanal and heptanal in human urine using magnetic solid-phase extraction coupled with in-situ derivatization by high-performance liquid chromatography. *Talanta* **2015**, *136*, 54–59. [CrossRef] [PubMed]
29. Palacios-López, D.L.; Prieto-Blanco, M.C.; Moliner-Martínez, Y.; Campins-Falcó, P. Carbonyl compounds-responsive 2,4-dinitrophenylhydrazine doped polydimethylsiloxane membrane as alternative derivatizing strategy prior to in-tube solid-phase microextraction coupled with capillary liquid chromatography analysis. *J. Chromatogr. A* **2025**, *1740*, 465595. [CrossRef]
30. Prieto-Blanco, M.C.; Jornet-Martínez, N.; Verdú-Andrés, J.; Molíns-Legua, C.; Campins-Falcó, P. Quantifying both ammonium and proline in wines and beer using a PDMS composite for sensoring. *Talanta* **2019**, *198*, 371–376. [CrossRef]
31. Prieto-Blanco, M.C.; Jornet-Martínez, N.; Moliner-Martínez, Y.; Molins-Legua, C.; Herráez-Hernández, R.; Verdú-Andrés, J.; Campins-Falcó, P. Development of a polydimethylsiloxane-thymol/nitroprusside composite based sensor involving thymol derivatization for ammonium monitoring in water samples. *Sci. Total Environ.* **2015**, *503–504*, 105–112. [CrossRef]
32. Yasin, T.; Zafar, M.S.; Albishi, H.M.; Eid, T.M.; Siddiqi, H.M.; Khan, M.U.A. Antibacterial and bioactive composite hydrogels from carrageenan-PVA-chitosan incorporated ZiF-8@GO for wound healing: In vitro and in vivo evaluations. *J. Biomater. Sci. Polym. Ed.* **2025**, *36*, 2237–2258. [CrossRef]
33. Ling, X.H.; Zhang, M.K.; Zhou, H.Y.; Han, G.Z. Preparation of a novel alginate hydrogel microspheres covered by hollow silica for controlled-release applications. *Eur. Polym. J.* **2024**, *204*, 112716. [CrossRef]
34. Begum, B.; Koduru, T.S.; Madni, S.N.; Fathima Anjum, N.; Seetharaman, S.; Veeranna, B.; Gupta, V.K. Dual-self-crosslinking effect of alginate-di-aldehyde with natural and synthetic co-polymers as injectable in situ-forming biodegradable hydrogels. *Gels* **2024**, *10*, 649. [CrossRef] [PubMed]
35. Sun, Y.; Wen, D.; Yuan, Q.; Wang, Y. Artificial synapses based on P(VDF-TrFE-CTFE)/sodium alginate heterojunction memristor for distance detection applications. *Mater. Today Nano* **2024**, *27*, 100490. [CrossRef]
36. Sundaraganesan, N.; Ayyappan, S.; Umamaheswari, H.; Joshua, B.D. FTIR, FT-Raman spectra and ab initio, DFT vibrational analysis of 2,4-dinitrophenylhydrazine. *Spectrochim. Acta A* **2007**, *66*, 17–27. [CrossRef]
37. Boumya, W.; Hammani, H.; Laghrib, F.; Lahrich, S.; Farahi, A.; Achak, M.; Mhammedi, M.A. Electrochemical study of 2,4-dinitrophenylhydrazine as derivatization reagent and aldehydes at carbon glassy electrode. *Electroanalysis* **2017**, *29*, 1700–1711. [CrossRef]
38. Adhikari, C.; Balasubramaniam, V.M.; Abbott, U.R. A rapid FTIR method for screening methyl sulfide and hexanal in modified atmosphere ready-to-eat entrees. *LWT-Food Sci. Technol.* **2003**, *36*, 21–27. [CrossRef]
39. Dwivedi, Y.; Rai, S.B. Spectroscopic study of overtone and combination bands in aliphatic aldehydes. *Vib. Spectrosc.* **2009**, *49*, 278–283. [CrossRef]
40. Zhao, X.; Yang, F.; Li, Z.; Tan, H. Formation and emission characteristics of PAHs during pyrolysis and combustion of coal and biomass. *Fuel* **2024**, *378*, 132935. [CrossRef]
41. Topolniak, I.; Gardette, J.L.; Thérias, S. Influence of zeolite nanoparticles on photostability of ethylene vinyl alcohol copolymer (EVOH). *Polym. Degrad. Stab.* **2015**, *121*, 137–148. [CrossRef]
42. Xu, M.Y.; Pei, X.Q.; Wu, Z.L. Identification and characterization of a novel "thermophilic-like" Old Yellow Enzyme from the genome of *Chryseobacterium* sp. CA49. *J. Mol. Catal. B Enzym.* **2014**, *108*, 64–71. [CrossRef]
43. Sivakumar, K.; Komathi, V.; Krishnan, M.M. Dinitrophenylhydrazine: β-cyclodextrin inclusion complex as a novel fluorescent chemosensor probe for Ce^{4+}. *Res. Chem. Intermed.* **2018**, *44*, 5301–5327. [CrossRef]
44. Stafiej, A.; Pyrzynska, K.; Ranz, A.; Lankmayr, E. Screening and optimization of derivatization in a heating block for the determination of aliphatic aldehydes by HPLC. *J. Biochem. Biophys. Methods* **2006**, *69*, 15–24. [CrossRef]
45. Polat, E.; Genç, A.N.; Güngör, F.Ş.; Altınbaş, M. Recovery of volatile fatty acids from anaerobic fermentation broth of baker's yeast industry effluent by liquid-liquid extraction. *J. Ind. Eng. Chem.* **2025**, *141*, 431–440. [CrossRef]
46. Poole, C.F. *Liquid-Phase Extraction*; Elsevier: Amsterdam, The Netherlands, 2019.
47. Huang, L.; Teng, H.; Wang, M.; Fang, J.; Yuan, Y.; Ma, M.; Guo, B. Isotope-coded derivatization with designed Girard-type reagent as charged isobaric mass tags for non-targeted profiling and discovery of natural aldehydes by liquid chromatography-tandem mass spectrometry. *J. Chromatogr. A* **2023**, *1702*, 464084. [CrossRef] [PubMed]
48. Goh, C.H.; Heng, P.W.S.; Chan, L.W. Alginates as a useful natural polymer for microencapsulation and therapeutic applications. *Carbohydr. Polym.* **2012**, *88*, 1–12. [CrossRef]
49. Tønnesen, H.H.; Karlsen, J. Alginate in drug delivery systems. *Drug Dev. Ind. Pharm.* **2002**, *28*, 621–630. [CrossRef]

50. Fang, Y.; Li, L.; Vreeker, R.; Yao, X.; Wang, J.; Ma, Q.; Phillips, G.O. Rehydration of dried alginate gel beads: Effect of the presence of gelatin and gum arabic. *Carbohydr. Polym.* **2011**, *86*, 1145–1150. [CrossRef]
51. Ching, S.H.; Bansal, N.; Bhandari, B. Alginate gel particles-A review of production techniques and physical properties. *Crit. Rev. Food Sci. Nutr.* **2017**, *57*, 1133–1152. [CrossRef]
52. Dossi, N.; Susmel, S.; Toniolo, R.; Pizzariello, A.; Bontempelli, G. Simultaneous determination of derivatized light aldehydes by microchip electrophoresis with electrochemical detection. *J. Chromatogr. A* **2008**, *1207*, 169–174. [CrossRef]
53. Liu, X.; Wang, S.; Tamogami, S.; Chen, J.; Zhang, H. An evaluation model for quality of frying oil using key aldehyde detected by HS-GC/MS. *Foods* **2022**, *11*, 2413. [CrossRef]
54. Wang, D.; Xiao, H.; Lyu, X.; Chen, H.; Wei, F. Lipid oxidation in food science and nutritional health: A comprehensive review. *Oil Crop Sci.* **2023**, *8*, 35–44. [CrossRef]
55. Hu, J.; Chen, S.-E.; Zhu, S.; Jia, W.; Sun, J.; Zhao, X.-E.; Liu, H. 13-Plex UHPLC-MS/MS analysis of hexanal and heptanal using multiplex tags chemical isotope labeling technology. *J. Am. Soc. Mass Spectrom.* **2020**, *31*, 1965–1973. [CrossRef] [PubMed]
56. Xia, L.; Du, Y.; Xiao, X.; Li, G. One-step membrane protected micro-solid-phase extraction and derivatization coupled to high-performance liquid chromatography for selective determination of aliphatic aldehydes in cosmetics and food. *Talanta* **2019**, *202*, 580–590. [CrossRef] [PubMed]
57. Qin, Y.; Li, H.; Luo, S.; Tang, S.; Zeng, H.; Zhu, S.; Ma, M. Rapid determination of α,β-unsaturated aldehydes in vegetable oils by desorption corona beam ionization-tandem mass spectrometry based on a twin derivatization strategy. *Microchem. J.* **2025**, *208*, 112447. [CrossRef]
58. Gabbanini, S.; Matera, R.; Valvassori, A.; Valgimigli, L. Rapid liquid chromatography-tandem mass spectrometry analysis of 4-hydroxynonenal for the assessment of oxidative degradation and safety of vegetable oils. *Anal. Chim. Acta* **2015**, *869*, 50–58. [CrossRef]
59. Bastos, L.C.S.; de Almeida Costa, E.A.; Pereira, P.A.P. Development, validation and application of an UFLC-DAD-ESI-MS method for determination of carbonyl compounds in soybean oil during continuous heating. *Food Chem.* **2017**, *218*, 518–524. [CrossRef]